



New family of 4-D hyperchaotic and chaotic systems with quadric surfaces of equilibria

Jay Prakash Singh ^{a,*}, Binoy Krishna Roy ^a, Sajad Jafari ^b

^a National Institute of Technology Silchar, Silchar, Assam, 788010, India

^b Ambikar University of Technology, Tehran, 15875-4413, Iran



ARTICLE INFO

Article history:

Received 1 January 2017

Revised 25 October 2017

Accepted 18 November 2017

Keywords:

Surface of equilibria

Hyperchaotic system

Chaotic system

Coexistence of attractors

Many equilibria chaotic system

Multi-stability

ABSTRACT

This paper reports 4-D hyperchaotic and chaotic systems with various quadric surfaces of equilibria. A known and systematic search procedure is used to generate the proposed systems. Six cases have non-degenerate quadric surfaces (ellipsoid, spheroid, sphere, elliptic hyperboloid of one sheet, circular hyperboloid of one sheet) type of equilibria and two cases have degenerate quadric surfaces (elliptic cylinder, circular cylinder) type of equilibria. All the cases in the new systems have coexistence of chaotic attractors. Chaotic natures of the new systems are confirmed by using various numerical tools. MATLAB simulation results are further validated by circuit implementations.

© 2017 Elsevier Ltd. All rights reserved.

1. Introduction

For a long time, it was supposed that the behaviour of a dynamical system depends on the characteristics of its equilibrium points [1] and the nature of equilibrium points depicts the applicability of the system [2]. Recently many chaotic/hyperchaotic systems are reported depending upon different shapes of their equilibrium points [3–5,6–9]. The investigation of different shape equilibrium points in four-dimensional chaotic systems is more interesting because 4-D systems are more complex than three-dimensional systems and have the ability to show some new types of behaviour like hyperchaos.

The available chaotic and hyperchaotic systems can be categorised into two parts: (i) self-excited attractors chaotic systems and (ii) hidden attractors chaotic systems [10–12]. A self-excited attractor has a basin of attraction that is associated with an unstable equilibrium, whereas a hidden attractor has a basin of attraction that does not intersect with small neighbourhoods of any equilibrium points [10–12]. The chaotic/hyperchaotic systems like Lorenz [13], Rossler [14], Lu [15], systems in [16,17], etc. have self-excited attractors [10,11]. The chaotic systems with stable equilibria only [18] or with no equilibria [19,20] are called hidden attractors chaotic systems [12,21–23]. Study of chaotic systems with hidden attractors is important because they can lead to unexpected

and disastrous behaviours with small changes in their dynamics as in aeroplane wing, electromechanical systems, bridge [1,2,22,24], etc. Many chaotic systems with an infinite number of equilibria (line/curve/plane-shaped equilibria) are also reported in the literature. The reported chaotic/hyperchaotic systems with many equilibria are classified in Table 1. It is noted from Table 1 that no 4-D chaotic/hyperchaotic system with a quadric surface of equilibria is reported in the literature.

Motivated by the above findings, this paper reports 4-D hyperchaotic and chaotic systems with quadric surfaces of equilibria. Two classes of chaotic systems with (i) only stable equilibria and (ii) no equilibria are considered under the category of hidden attractors in [24]. Recently, many chaotic systems with infinitely many equilibria are also reported in the literature [41] [24,26,42]. The contributions and novelty of this paper when compared with the available literature, are as given below:

- (i) three cases with hyperchaotic and five cases with chaotic attractors in 4-D systems with various quadric surfaces of equilibria are developed,
- (ii) six cases have non-degenerate real quadric surfaces (ellipsoid, paraboloid, and hyperboloid) [43] type of equilibria and two cases have degenerate quadric surfaces (cylinder) [43] type of equilibria,
- (iii) all the eight cases in the three new systems show coexistence of chaotic attractors,
- (iv) one of the cases in the proposed systems exhibits an infinite number of attractors.

* Corresponding author.

E-mail addresses: 12-23-204@student.nits.ac.in (J.P. Singh), sajadjafari@aut.ac.ir, bkr@nits.ac.in (S. Jafari).

Table 1

Categorisation of the reported chaotic and hyperchaotic systems with an infinite number of equilibrium points.

Sl. No.	3-D/4-D System	Nature of system	Reference of the papers
1.	3-D Chaotic system	Line of equilibria	[4,25,26]
		Many equilibria	[27]
		Circle of equilibria	[3,5,28–30]
		Surface of equilibria	[1]
		Curve of equilibria	[31,32]
		Square shaped equilibria	[5,30,33]
		Ellipse shaped equilibria	[5]
		Sphere of equilibria	[34]
2.	4-D Chaotic system	Plane of equilibria	[35]
		Quadric surfaces of equilibria	The present work
3.	4-D Hyperchaotic system	Line of equilibria	[36,37]
		Curve of equilibria	[38]
		Quadric surfaces of equilibria	The present work
4.	4-D Memristive hyperchaotic system	Line of equilibria	[39,40]

Rest of the paper is organised as follows. **Section 2** represents the dynamic formulation of the new systems. Stability analysis of equilibrium points of the three cases of the new systems is discussed in **Section 3**. Numerical analyses and MATLAB simulations are done to confirm the chaotic behaviours of the proposed systems in **Section 4**. Circuit design and implementation of Cases QS1, QS5 and QS6 of the new systems are presented in **Section 5**. The paper is concluded in **Section 6**.

2. Dynamics of the new systems with quadric surfaces of equilibria

A dissipative dynamical system may exhibit chaotic behaviour if it satisfies the following fundamental dynamical properties [44,45]:

- (i) There should be at least one nonlinear/piecewise-linear terms in a system.
- (ii) Its dimension must be greater than two.
- (iii) The divergence of the system should decay exponentially, i.e. the volume of the system shrinks exponentially to zero with respect to time.
- (iv) The sum of the trace of the Jacobian matrix of the system must be less the zero.

A dissipative dynamical system produces hyperchaotic behaviour if it satisfies the above-stated fundamental properties (i), (iii) and (iv) and its dimension must be greater than three.

The references [28,42] proposed a dimensionless third order differential equation with an infinite number of equilibria whose dynamics is described in (1).

$$\begin{cases} \dot{x}_1 = ax_3 \\ \dot{x}_2 = x_3 f_1(x_1, x_2, x_3) \\ \dot{x}_3 = x_1^2 + x_2^2 - r^2 + x_3 f_2(x_1, x_2, x_3) \end{cases} \quad (1)$$

where a and r are the parameters and $f_1(x_1, x_2, x_3), f_2(x_1, x_2, x_3)$ are the nonlinear functions.

As an extension of the system in (1), Gotthans et al. [30] proposed a simple 3-D chaotic system with a circle of equilibria. This system [30] is described in (2).

$$\begin{cases} \dot{x}_1 = x_3 \\ \dot{x}_2 = -x_3(ax_2 + bx_2^2 + x_1x_3) \\ \dot{x}_3 = x_1^2 + x_2^2 - 1 \end{cases} \quad (2)$$

The system in (2) is chaotic with the value of parameters $a = 5$, $b = 3$ and at initial conditions $x(0) = (0, 0, 0)^T$ [30].

Motivated by the above extension and considering the fundamental dynamical properties stated above, this paper presents three hyperchaotic systems with quadric surfaces of equilibria. A known and widely used systematic search procedure is used in the paper as in [42,46–49]. The general expression of the proposed

new 4-D hyperchaotic and chaotic systems with quadric surfaces of equilibria is given in (3).

$$\begin{cases} \dot{x}_1 = x_3 \\ \dot{x}_2 = -x_3(ax_2 + bx_2^2 + x_1x_3) \\ \dot{x}_3 = f_1(x_1, x_2, x_4) - 1 \\ \dot{x}_4 = x_3 f_2(x_2, x_4) \end{cases} \quad (3)$$

where $f_1(x_1, x_2, x_4)$ is a nonlinear function, and $f_2(x_2, x_4)$ is a linear function. Different choices of $f_1(x_1, x_2, x_4)$ and $f_2(x_2, x_4)$ lead to system with various quadric surfaces of equilibria. With suitable choices of the functions $f_1(x_1, x_2, x_4)$ and $f_2(x_2, x_4)$, three systems are developed to show the quadric surface of equilibria. Hence, the parameters of the systems are chosen in such a manner that their equilibria follow the standard equations of quadric surfaces [50,51]. These systems are given in (4)–(6).

$$\begin{cases} \dot{x}_1 = x_3 \\ \dot{x}_2 = -x_3(hx_2 + dx_2^2 + x_1x_3) \\ \dot{x}_3 = \frac{x_1^2}{a^2} + \frac{x_2^2}{b^2} + \frac{x_4^2}{c^2} - 1 \\ \dot{x}_4 = -gx_3x_4 \end{cases} \quad (4)$$

$$\begin{cases} \dot{x}_1 = x_3 \\ \dot{x}_2 = -x_3(hx_2 + dx_2^2 + x_1x_3) \\ \dot{x}_3 = \frac{x_1^2}{a^2} + \frac{x_2^2}{b^2} - \frac{x_4^2}{b^2} - 1 \\ \dot{x}_4 = -gx_2x_3 \end{cases} \quad (5)$$

$$\begin{cases} \dot{x}_1 = x_3 \\ \dot{x}_2 = -x_3(hx_2 + dx_2^2 + x_1x_3) \\ \dot{x}_3 = \frac{x_1^2}{a^2} + \frac{x_2^2}{b^2} - 1 \\ \dot{x}_4 = -gx_3x_4 \end{cases} \quad (6)$$

The systems in (4)–(6) are simulated using the numerical method with fixed initial conditions to observe (i) an aperiodic or unpredictable nature of time series of the states and (ii) the presence of an irregular shape or distinct curve in the phase plane/space. The occurrence of these phenomena is an indication of chaotic behaviour of the systems. Another important property of a chaotic system is that it is highly sensitive to initial conditions. This property is tested for the proposed systems and it is shown that with the change of initial conditions the systems have a co-existing pair of attractors and other behaviours. Further, Lyapunov exponents (LEs) are calculated to confirm the chaotic/hyperchaotic nature of the systems. Chaotic and hyperchaotic systems have (+, 0, −) and (+, +, 0, −) sign of Lyapunov exponents, respectively. Lyapunov exponents are the quantitative indication of hyperchaotic, chaotic and other dynamical behaviours [52]. Various combinations of $f_1(x_1, x_2, x_4)$ and $f_2(x_2, x_4)$ are considered to generate the proposed hyperchaotic/chaotic systems so that the first LE is at least greater than 0.2.

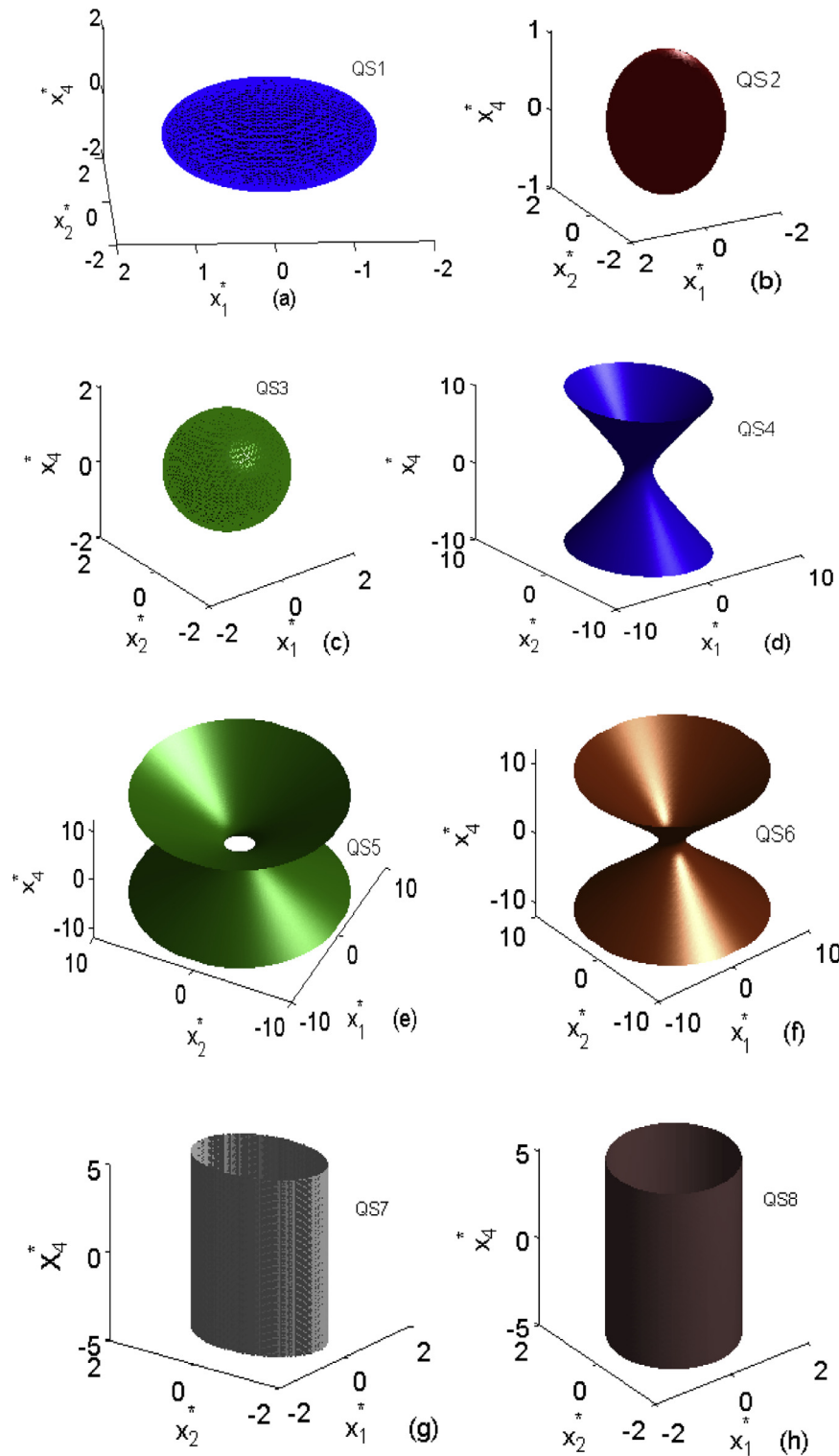


Fig. 1. Shapes of the equilibria of the cases given in Table 2.

Using three systems (4)–(6), eight different cases are developed to show the quadric surface of equilibria with hyperchaotic and chaotic behaviour. Among eight cases, three cases show hyperchaotic behaviour and five cases show chaotic behaviour. These are named as QS1 to QS8, and the details are shown in Table 2. Cases QS1, QS2, QS3, QS4 and QS6 belong to system (4), Case QS5 belongs to system (5) and Cases QS7 and QS8 belong to system (6). The first six Cases (QS1 to QS6) have non-degenerate real

quadric surfaces (ellipsoid, spheroid, and hyperboloid) [43,50] type of equilibria and the rest two Cases (QS7 and QS8) have degenerate quadric surfaces (cylinder) [43] type of equilibria. Out of eight cases, three Cases namely QS1, QS4 and QS7 are hyperchaotic and the rest five cases are chaotic. Table 2 describes the systems' dynamics, location of equilibria, shape of equilibria, Lyapunov exponents, nature of the systems, Lyapunov dimension/Kaplan-Yorke dimension (D_{KY}) and initial conditions used for simulation of these

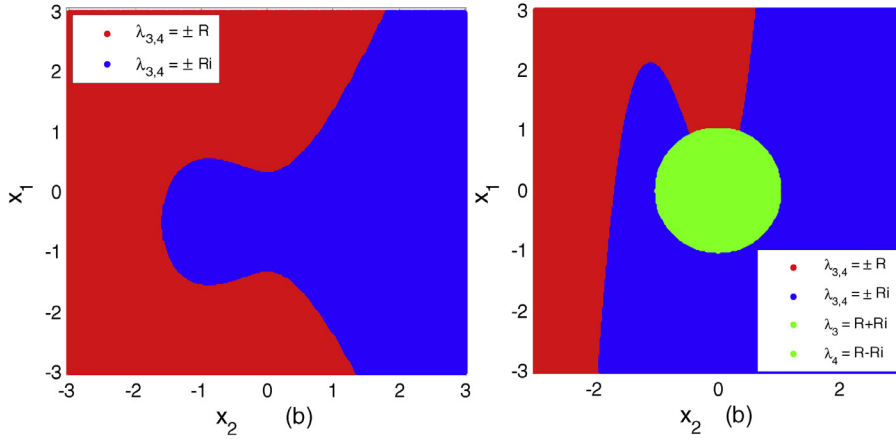


Fig. 2. Eigenvalues of Cases: (a) QS1 and (b) QS5 for equilibrium point $E3$ and $E3$, respectively.

Table 2

Three hyperchaotic and five chaotic Cases of systems (4)–(6) with quadric surfaces of equilibria.

Case	System dynamics	Equilibria	Shape	LEs and nature	D_{KY}	Initial condition
Non-degenerate real quadric surfaces						
QS1	$\dot{x}_1 = x_3 \quad \dot{x}_2 = -x_3(hx_2 + dx_2^2 + x_1x_3) \quad \dot{x}_3 = \left(\frac{x_1^2}{a^2} + \frac{x_2^2}{b^2} + \frac{x_3^2}{c^2} = 1, x_3 = 0\right)$ $\frac{x_1^2}{a^2} + \frac{x_2^2}{b^2} + \frac{x_3^2}{c^2} - 1 \quad \dot{x}_4 = -gx_3x_4 \quad h = 5, d = 3, g = 1, \frac{1}{a^2} = 2.7, b = 1, 1/c^2 = 1.5$	Ellipsoid	$LE = \begin{pmatrix} 0.0684 \\ 0.0047 \\ 0 \\ -0.2542 \end{pmatrix}$ and hyperchaotic	3.28	$x(0) = \begin{pmatrix} 0.1 \\ 0.01 \\ 0.01 \\ 0.1 \end{pmatrix}^T$	
QS2	$\dot{x}_1 = x_3 \quad \dot{x}_2 = -x_3(hx_2 + dx_2^2 + x_1x_3) \dot{x}_3 = \left(\frac{x_1^2}{a^2} + \frac{x_2^2}{a^2} + \frac{x_3^2}{b^2} = 1, x_3 = 0\right)$ $\frac{x_1^2}{a^2} + \frac{x_2^2}{a^2} + \frac{x_3^2}{b^2} - 1 \quad \dot{x}_4 = -gx_3x_4 \quad h = 5, d = 3, g = 1, a = 1, 1/b^2 = 2$	Spheroid	$LE = \begin{pmatrix} 0.0403 \\ 0 \\ -0.0024 \\ -0.0909 \end{pmatrix}$ and chaotic	3.41	$x(0) = \begin{pmatrix} 0.1 \\ 0.01 \\ 0.01 \\ 0.1 \end{pmatrix}^T$	
QS3	$\dot{x}_1 = x_3 \quad \dot{x}_2 = -x_3(hx_2 + dx_2^2 + x_1x_3) \dot{x}_3 = \left(\frac{x_1^2}{a^2} + \frac{x_2^2}{a^2} + \frac{x_3^2}{a^2} = 1, x_3 = 0\right)$ $\frac{x_1^2}{a^2} + \frac{x_2^2}{a^2} + \frac{x_3^2}{a^2} - 1 \quad \dot{x}_4 = -gx_3x_4 \quad h = 5, d = 3, g = 1, a = 1$	Sphere	$LE = \begin{pmatrix} 0.03547 \\ 0 \\ -0.0030 \\ -0.0776 \end{pmatrix}$ and chaotic	3.42	$x(0) = \begin{pmatrix} 0.1 \\ 0.01 \\ 0.01 \\ 0.1 \end{pmatrix}^T$	
QS4	$\dot{x}_1 = x_3 \quad \dot{x}_2 = -x_3(hx_2 + dx_2^2 + x_1x_3) \dot{x}_3 = \left(\frac{x_1^2}{a^2} + \frac{x_2^2}{b^2} - \frac{x_3^2}{c^2} = 1, x_3 = 0\right)$ $\frac{x_1^2}{a^2} + \frac{x_2^2}{b^2} - \frac{x_3^2}{c^2} - 1 \quad \dot{x}_4 = -gx_3x_4 \quad h = 5, d = 3, g = 1, 1/a^2 = 2.5, b = 1, 1/c^2 = 2.5$	Elliptic hyperboloid of one sheet	$LE = \begin{pmatrix} 0.08756 \\ 0.0036 \\ 0 \\ -0.264 \end{pmatrix}$ and hyperchaotic	3.34	$x(0) = \begin{pmatrix} 0.01 \\ 0.01 \\ 0.01 \\ 0.1 \end{pmatrix}^T$	
QS5	$\dot{x}_1 = x_3 \quad \dot{x}_2 = -x_3(hx_2 + dx_2^2 + x_1x_3) \dot{x}_3 = \left(\frac{x_1^2}{a^2} + \frac{x_2^2}{a^2} - \frac{x_3^2}{b^2} = 1, x_3 = 0\right)$ $\frac{x_1^2}{a^2} + \frac{x_2^2}{a^2} - \frac{x_3^2}{b^2} - 1 \quad \dot{x}_4 = -gx_2x_3 \quad h = 5, d = 3, g = 0.01, a = 1, b = 1$	Circular hyperboloid of one sheet	$LE = \begin{pmatrix} 0.0312 \\ 0 \\ -0.0014 \\ -0.0737 \end{pmatrix}$ and chaotic	3.40	$x(0) = \begin{pmatrix} 0.01 \\ 0.01 \\ 0.01 \\ 0.1 \end{pmatrix}^T$	
QS6	$\dot{x}_1 = x_3 \quad \dot{x}_2 = -x_3(hx_2 + dx_2^2 + x_1x_3) \dot{x}_3 = \left(\frac{x_1^2}{a^2} + \frac{x_2^2}{a^2} - \frac{x_3^2}{b^2} = 1, x_3 = 0\right)$ $\frac{x_1^2}{a^2} + \frac{x_2^2}{a^2} - \frac{x_3^2}{b^2} - 1 \quad \dot{x}_4 = -gx_3x_4 \quad h = 5, d = 3, g = 1, a = 1, 1/b^2 = 0.5$	Circular hyperboloid of one sheet	$LE = \begin{pmatrix} 0.03080 \\ 0 \\ -0.0028 \\ -0.0686 \end{pmatrix}$ and chaotic	3.40	$x(0) = \begin{pmatrix} 0.01 \\ 0.01 \\ 0.01 \\ 0.1 \end{pmatrix}^T$	
Degenerate quadric surfaces						
QS7	$\dot{x}_1 = x_3 \quad \dot{x}_2 = -x_3(hx_2 + dx_2^2 + x_1x_3) \dot{x}_3 = \left(\frac{x_1^2}{a^2} + \frac{x_2^2}{b^2} = 1, x_3 = 0\right)$ $\frac{x_1^2}{a^2} + \frac{x_2^2}{b^2} - 1 \quad \dot{x}_4 = -gx_3x_4 \quad h = 5, d = 3, g = 1, \frac{1}{a^2} = 2.78, b = 1$	Elliptic cylinder	$LE = \begin{pmatrix} 0.1005 \\ 0.0040 \\ 0 \\ -0.2881 \end{pmatrix}$ and hyperchaotic	3.36	$x(0) = \begin{pmatrix} 0.01 \\ 0.01 \\ 0.01 \\ 0.1 \end{pmatrix}^T$	
QS8	$\dot{x}_1 = x_3 \quad \dot{x}_2 = -x_3(hx_2 + dx_2^2 + x_1x_3) \dot{x}_3 = \frac{x_1^2}{a^2} + \left(\frac{x_1^2}{a^2} + \frac{x_2^2}{a^2} = 1, x_3 = 0\right)$ $\frac{x_1^2}{a^2} - 1 \quad \dot{x}_4 = -gx_3x_4 \quad h = 6, d = 3, g = 1, a = 1$	Circular cylinder	$LE = \begin{pmatrix} 0.0337 \\ 0 \\ -0.0030 \\ -0.0714 \end{pmatrix}$ and chaotic	3.42	$x(0) = \begin{pmatrix} 0.01 \\ 0.01 \\ 0.01 \\ 0.1 \end{pmatrix}^T$	

Table 3

Some possible equilibrium points and eigenvalues of Case QS1 with $p = \frac{1}{a^2} = 2.7$, $q = \frac{1}{b^2} = 1$, $r = \frac{1}{c^2} = 1.5$, $h = 5$, $d = 3$, $g = 1$, $R > 0$.

Equilibrium Point	Eigenvalues	Case	Nature
$E1 = (x_1, 0, 0, \sqrt{\frac{-(px_1^2 - 1)}{r}})$	$\lambda_{1,2} = 0$ $\lambda_{3,4} = \pm\sqrt{0.2}(\sqrt{27(x_1^*)^2 + 27x_1^* - 1})$	$x_1^* \geq 0.358, \lambda_{3,4} = \pm R$ $x_1^* = 0, \lambda_{3,4} = \mp\sqrt{0.2}i$ $-1.035 < x_1^* < 0.035, \lambda_{3,4} = \pm Ri$ $x_1^* \leq -1.035, \lambda_{3,4} = \pm R$	Saddle Non-hyperbolic Non-hyperbolic Saddle
$E2 = (\sqrt{\frac{-(qx_2^2 - 1)}{r}}, x_2, 0, 0)$	$\lambda_{1,2} = 0$ $\lambda_{3,4} = \pm\sqrt{3.286\sqrt{1 - (x_2^*)^2} - 6(x_2^*)^3 - 10(x_2^*)^2}$	$0.478 < x_2^* \leq 1, \lambda_{3,4} = \pm Ri$ $x_2^* > 1, \lambda_{3,4} = R \pm Ri$ $-0.638 \leq x_2^* \leq 0.478, \lambda_{3,4} = \pm R$ $-1 < x_2^* < -0.638, \lambda_{3,4} = \pm Ri$ $x_2^* \leq -1, \lambda_{3,4} = R \pm Ri$	Non-hyperbolic Saddle focus Saddle Non-hyperbolic Saddle focus
$E3 = (x_1, x_2, 0, \sqrt{\frac{-(px_1^2 + qx_2^2 - 1)}{r}})$	$\lambda_{1,2} = 0$ $\lambda_{3,4} = \pm\sqrt{12.07(x_1^*)^2 + 12.07x_1^* - 17.89(x_2^*)^2 - 13.4164(x_2^*)^3 - 4.472}$	Natures of eigenvalues for different values of state variables are shown in Fig. 2(a). It is seen that in this case, the system has saddle and non-hyperbolic types of equilibria	

Table 4

Some possible equilibrium points and eigenvalues of Case QS5 with $h = 5$, $d = 3$, $g = 0.01$, $R > 0$ and $p = \frac{1}{a^2} = 1$, $r = \frac{1}{b^2} = 1$.

Equilibrium Point	Eigenvalues	Case	Nature
$E1 = (x_1, 0, 0, \sqrt{(x_1^2 - 1)})$	$\lambda_{1,2} = 0$ $\lambda_{3,4} = \pm(\sqrt{2x_1^*})$	$x_1^* > 0, \lambda_{3,4} = \pm R$ $x_1^* = 0, \lambda_{3,4} = 0$ $x_1^* < 0, \lambda_{3,4} = \pm Ri$	Saddle Non-hyperbolic Non-hyperbolic
$E2 = (x_1, -\frac{h}{d}, 0, \frac{1}{d}\sqrt{d^2x_1^2 - d^2 + h^2})$	$\lambda_{1,2} = 0$ $\lambda_{3,4} = \pm\sqrt{2x_1^* + 0.011\sqrt{9(x_1^*)^2 + 16}}$	$x_1^* > -0.0222, \lambda_{3,4} = \pm R$ $x_1^* \leq -0.0222, \lambda_{3,4} = \pm Ri$	Saddle Non-hyperbolic
$E3 = (x_1^*, x_2^*, 0, \sqrt{(x_1^*)^2 + (x_2^*)^2 - 1})$	$\lambda_{1,2} = 0$ $\lambda_{3,4} = \pm\sqrt{-10(x_2^*)^2 + 2x_1^* - 6(x_2^*)^3 + 0.02 x_2^*\sqrt{(x_1^*)^2 + (x_2^*)^2 - 1}}$	Natures of eigenvalues for different values of state variables x_1^*, x_2^* are shown in Fig. 2(b). It is observed that the QS5 Case for E3 equilibrium points has saddle, non-hyperbolic and saddle-foci types of equilibria.	

Table 5

Some possible equilibrium points and eigenvalues of Case QS7 with $h = 5$, $d = 3$, $g = 1$, $R > 0$ and $p = \frac{1}{a^2} = 2.7$, $q = \frac{1}{b^2} = 1$.

Equilibrium Point	Eigenvalues	Case	Nature
$E1 = (0.608, 0, 0, x_4^*)$	$\lambda_{1,2} = 0$ $\lambda_{3,4} = \pm 1.8128$		Saddle
$E2 = (x_1^*, \sqrt{-(px_1^*)^2 - 1}/q, 0, 0)$	$\lambda_{1,2} = 0$ $\lambda_{3,4} = \pm\sqrt{\frac{-1119 + 1630.0x_1^* + 1119(x_1^*)^2}{-670.82\sqrt{-0.37(x_1^*)^2 + 0.37} + 670.82(x_1^*)^2\sqrt{-2.7(x_1^*)^2 + 0.37}}}$	$0.586 \leq x_1^* \leq 1, \lambda_{3,4} = \pm R$ $-1 \leq x_1^* \leq 0.58, \lambda_{3,4} = \pm Ri$ $x_1^* < -1, x_1^* > 1, \lambda_{3,4} = R \pm Ri$	Saddle Non-hyperbolic Saddle focus
$E3 = (\sqrt{-(qx_2^*)^2 - 1}/p, x_2^*, 0, 0)$	$\lambda_{1,2} = 0$ $\lambda_{3,4} = \pm\sqrt{\frac{3.286\sqrt{-(x_2^*)^2 - 1}}{-6(x_2^*)^3 - 10(x_2^*)^2}}$	$-0.637 \leq x_2^* \leq 0.476, \lambda_{3,4} = \pm R$ $0.476 < x_2^* < 1, \lambda_{3,4} = \pm Ri$ $-1 \leq x_2^* \leq -0.638, \lambda_{3,4} = \pm Ri$ $x_2^* < -1, x_2^* > 1, \lambda_{3,4} = R \pm Ri$	Saddle Non-hyperbolic Non-hyperbolic Saddle focus
$E4 = (\sqrt{-(qx_2^*)^2 - 1}/p, x_2^*, 0, x_4^*)$	$\lambda_{1,2} = 0$ $\lambda_{3,4} = \pm\sqrt{\frac{3.286\sqrt{-(x_2^*)^2 - 1}}{-6(x_2^*)^3 - 10(x_2^*)^2}}$	$-0.637 \leq x_2^* \leq 0.476, \lambda_{3,4} = \pm R$ $0.476 < x_2^* < 1, \lambda_{3,4} = \pm Ri$ $-1 \leq x_2^* \leq -0.638, \lambda_{3,4} = \pm Ri$ $x_2^* < -1, x_2^* > 1, \lambda_{3,4} = R \pm Ri$	Saddle Non-hyperbolic Non-hyperbolic Saddle focus

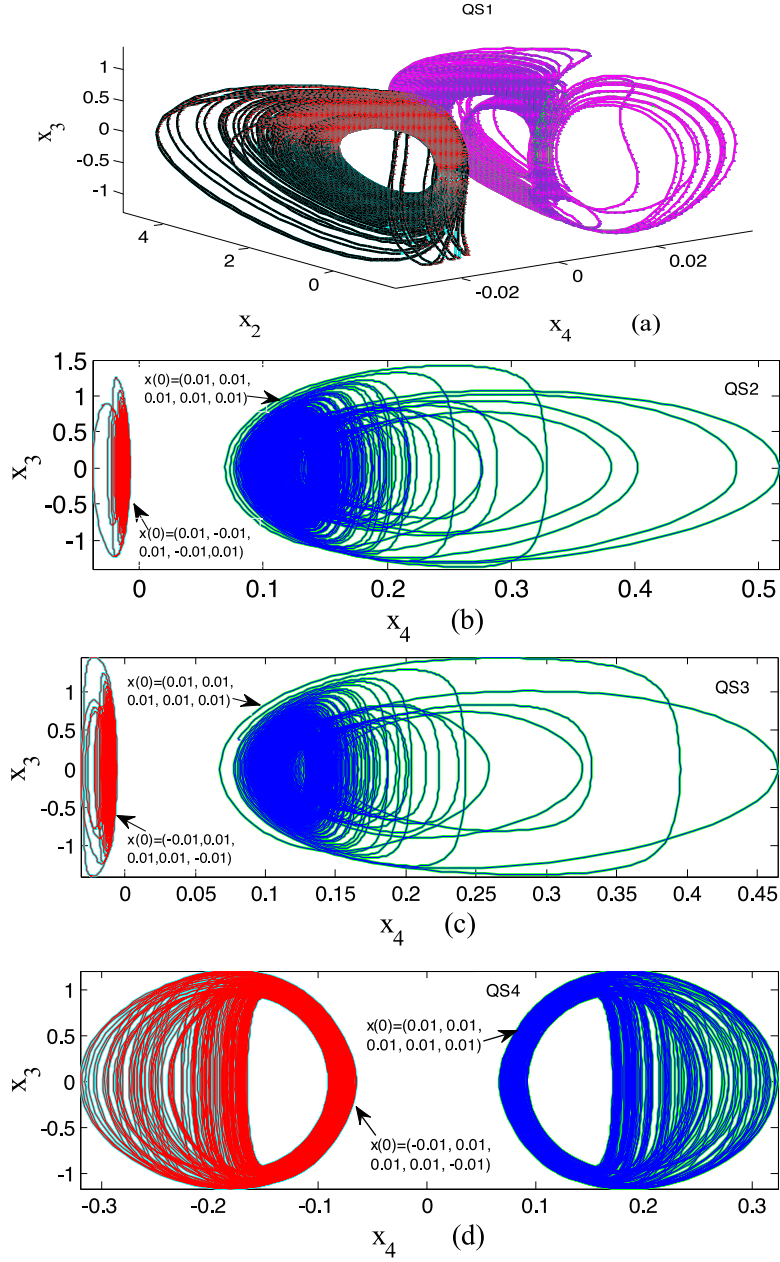


Fig. 3. Coexistence of chaotic attractors of the cases of systems given in Table 2, where $x(0) = (\pm 0.01, 0.01, 0.01, \pm 0.01)^T$ for QS1, QS3–8 and $x(0) = (\pm 0.01, 0.01, \pm 0.01, 0.01)^T$ for QS2.

Cases. The shapes of equilibria of the eight cases from the three proposed systems are shown in Fig. 1.

3. Stability analysis of equilibrium points

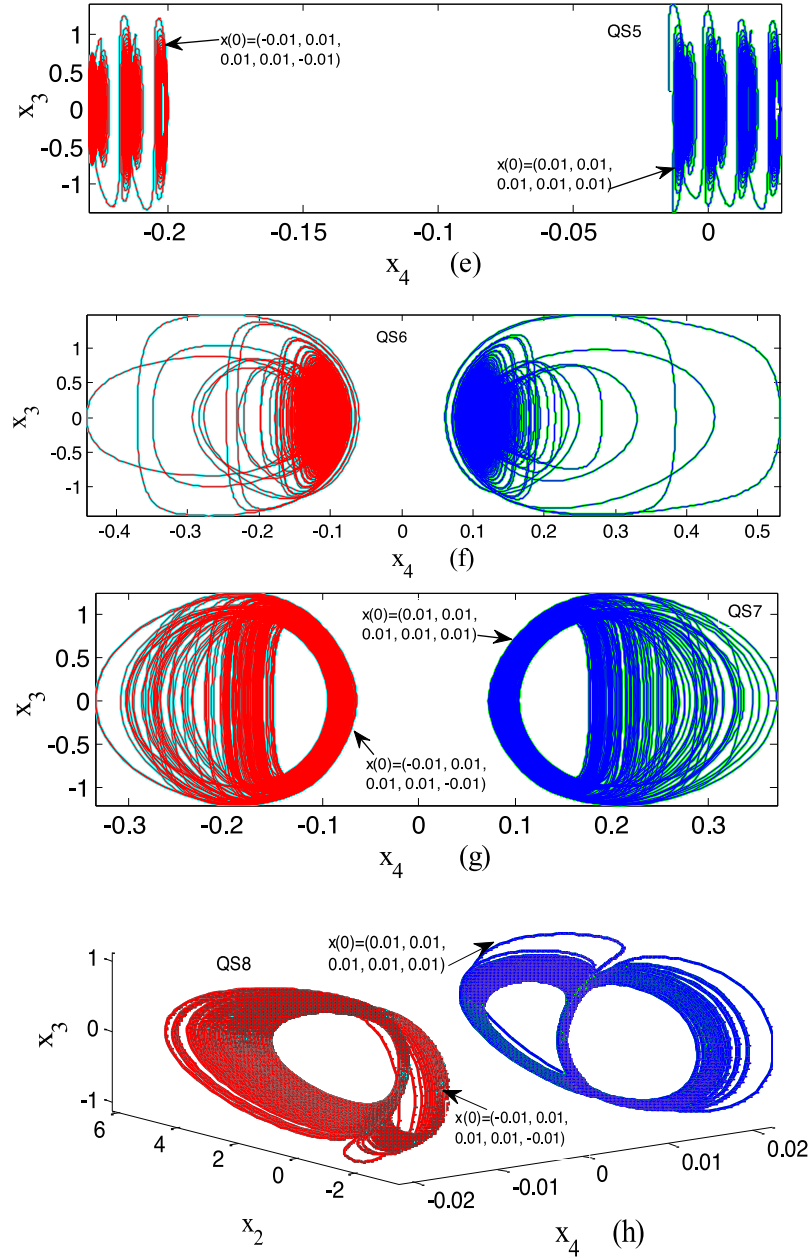
This section describes the stability analysis of the equilibrium points of the cases of systems given in Table 2. Out of the eight cases, three Cases QS1, QS5 and QS7 are considered for the stability analyses. The stability analysis of the equilibrium points of the rest five cases can also be done in a similar manner.

3.1. Equilibrium points and eigenvalues of case QS1

The Jacobian matrix used for finding the eigenvalues of Case QS1 with $p = \frac{1}{a^2}$, $q = \frac{1}{b^2}$, $r = \frac{1}{c^2}$ is given in (7).

$$J = \begin{bmatrix} 0 & 0 & 1 & 0 \\ -(x_3^*)^2 & -h(x_3^*) - 2d(x_2^*)(x_3^*) & -(h(x_2^*) + d(x_2^*)^2 + 2(x_1^*)(x_3^*)) & 0 \\ 2p(x_1^*) & 2q(x_2^*) & 0 & 2r(x_4^*) \\ 0 & 0 & -g(x_4^*) & -g(x_3^*) \end{bmatrix} \quad (7)$$

As mentioned in Table 2, Case QS1 has equilibria as $px_1^2 + qx_2^2 + rx_4^2 = 1, x_3 = 0$. Using these, various locations of equilibrium points can be obtained. Here, four such cases are considered to show the stability of the equilibria. The equilibrium points and eigenvalues of Case QS1 using (7), as a function of state variables, are given in the first and second columns of Table 3, respectively. It is seen that the eigenvalues $(\lambda_{3,4})$ are the function of either state variables x_1^* or x_2^* or (x_1^*, x_2^*) . Thus, sign of $(\lambda_{3,4})$ depends on the values of state variables. To discuss on the sign of the eigenvalues $(\lambda_{3,4})$, different possible cases are considered in the third column of Table 3.

**Fig. 3.** Continued

The nature of the equilibrium points for different cases of eigenvalues are shown in the fourth column of **Table 3**. Two types of nature of the equilibrium points are observed in Case QS1. These are saddle-point and non-hyperbolic. In **Table 3**, R is considered as a positive constant.

3.2. Equilibrium points and eigenvalues of case QS5

The Jacobian matrix of case QS5 with $p = \frac{1}{a^2}$, $r = \frac{1}{b^2}$ is written in (8).

$$J = \begin{bmatrix} 0 & 0 & 1 & 0 \\ -(x_3^*)^2 & -h(x_3^*) - 2d(x_2^*)(x_3^*) & -(h(x_2^*) + d(x_2^*)^2 + 2(x_1^*)(x_3^*)) & 0 \\ 2p(x_1^*) & 2p(x_2^*) & 0 & -2r(x_4^*) \\ 0 & -g(x_3^*) & -g(x_2^*) & 0 \end{bmatrix} \quad (8)$$

As mention in **Table 2**, Case QS5 has equilibria as $(px_1^2 + px_2^2 - rx_4^2 = 1, x_3 = 0)$, where $p = r = 1$. Using these, various locations of equilibrium points are obtained. Three possible cases are considered here to show the stability of the equilibria of Case QS5. The equilibrium points, eigenvalues and nature of Case QS5 using Jacobian (8) are given in **Table 4**. It may be noted that the eigenvalues $(\lambda_{3,4})$ are the function of state variables x_1^* or x_2^* or $(x_1^* \text{ and } x_2^*)$. The nature of the equilibrium points for different cases of eigenvalues is shown in the fourth column of **Table 4**. It is observed that the nature of the equilibrium points are either saddle point or non-hyperbolic in Case QS5.

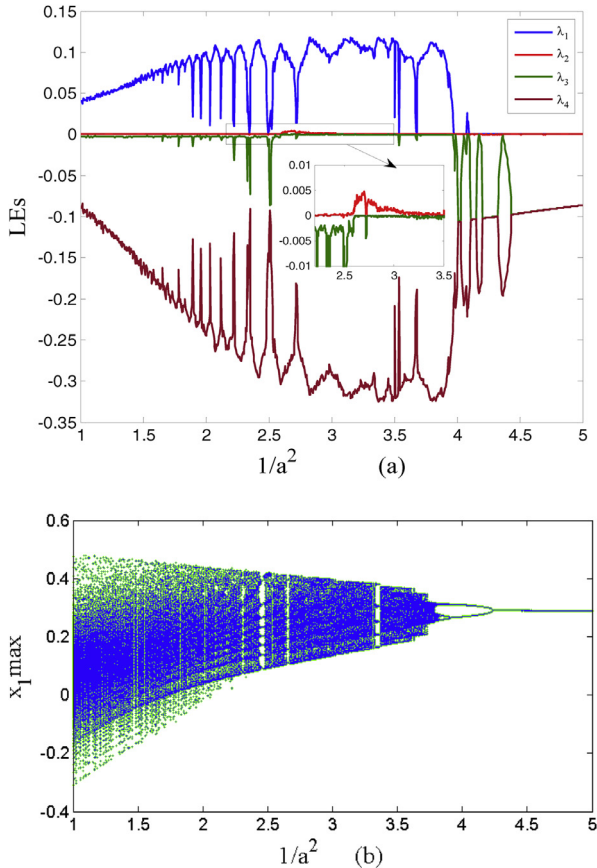


Fig. 4. Lyapunov spectrums and bifurcation diagram of QS1 Case with $x(0) = (0.01, 0.01, 0.01, 0.01)^T$.

3.3. Equilibrium points and eigenvalues of case QS7

The Jacobian matrix of case QS7 with $p = \frac{1}{a^2}$, $q = \frac{1}{b^2}$ is written in (9).

$$J = \begin{bmatrix} 0 & 0 & 1 & 0 \\ -(x_3^*)^2 & -h(x_3^*) - 2d(x_2^*)(x_3^*) & -\left(h(x_2^*) + d(x_2^*)^2 + 2(x_1^*)(x_3^*)\right) & 0 \\ 2p(x_1^*) & 2q(x_2^*) & 0 & 0 \\ 0 & 0 & -g(x_4^*) & -g(x_3^*) \end{bmatrix} \quad (9)$$

As noted in Table 2, Case QS7 has equilibria as $(2.7x_1^2 + x_2^2 = 1, x_3 = 0)$. For Case QS7, four possible types of equilibrium points are considered to discuss their stability. The location of equilibrium points, eigenvalues and nature of Case QS7 using Jacobian (9) are given in Table 5. Considering the different possible values of the state variables, the eigenvalues and nature

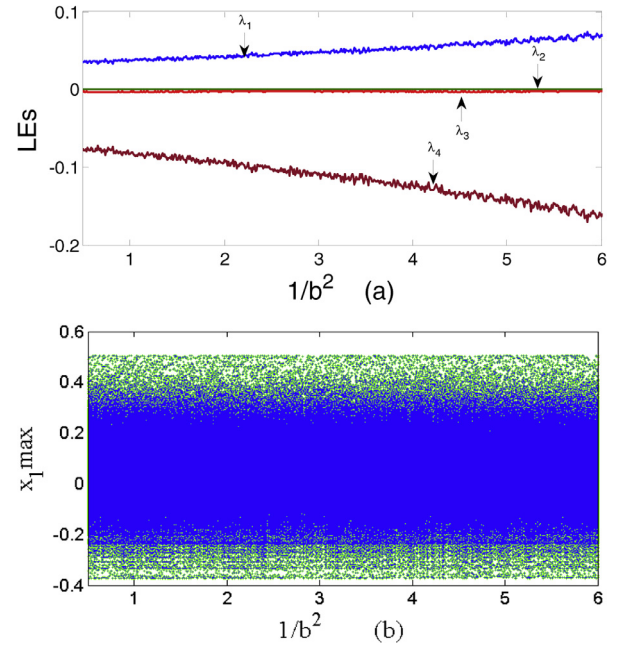


Fig. 5. Lyapunov spectrums and bifurcation diagram of QS2 Case with $x(0) = (0.01, 0.01, 0.01, 0.01)^T$.

of equilibria are shown in Table 5. The nature of the equilibrium points are saddle point and non-hyperbolic in Case QS7 also.

4. Numerical validation of chaotic behaviours of cases of the systems given in Table 2

The hyperchaotic and chaotic attractors of all the eight systems are shown in Fig. 3. The attractors in Fig. 3 are generated with $T = 2000$ observation time but ignoring the initial transient time (till $T = 1500$) in MATLAB-14a simulation environment. The parameters given in Table 2 are considered for plotting the chaotic and hyperchaotic attractors. It is observed from Fig. 3 that the proposed systems have coexistence of attractors and Case QS5 has coexistence of multiple attractors.

The cases of the systems (4)–(6) presented in Table 2 are similar in structure. However, based on the LEs as given in Table 2, Cases QS1, QS4 and QS7 are hyperchaotic and the rest five cases are chaotic. The complex dynamic behaviours of QS1, a hyperchaotic case, and QS2, a chaotic case, are only presented in details to avoid the repetitions of similar figures. Lyapunov spectrum and bifurcation diagram of Cases QS1 and QS2 are shown in Figs. 4 and 5, respectively. Lyapunov exponents of a hyperchaotic/chaotic system are sensitive to both the sampling time and observation time [53]. The best results are observed with relatively larger obser-

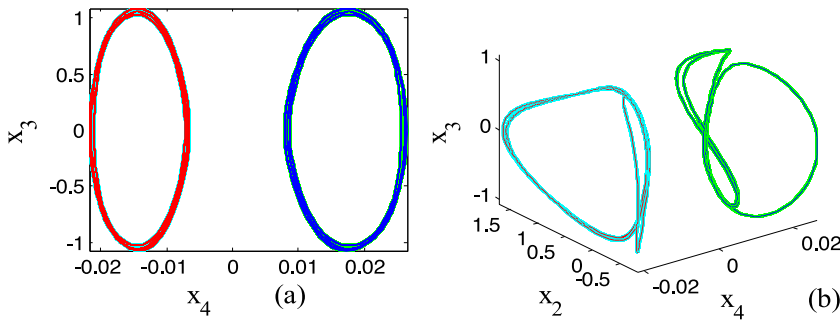


Fig. 6. Coexistence of periodic orbits of QS1 Case with $x(0) = (\pm 0.1, 0.01, 0.01, \pm 0.01)^T$ and $1/a^2 = 4.5$.

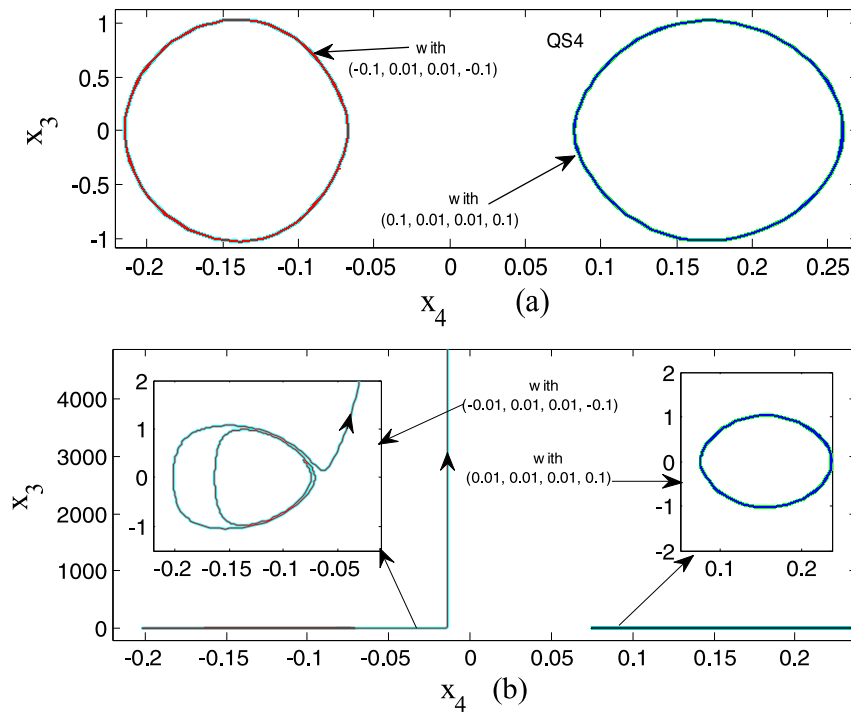


Fig. 7. (a) Coexistence of periodic orbits with $x(0) = (\pm 0.1, 0.01, \pm 0.01, 0.1)^T$ and (b) coexistence of periodic orbit and infinitely going trajectory with $x(0) = (\pm 0.01, 0.01, \pm 0.01, 0.1)^T$ of Case QS4.

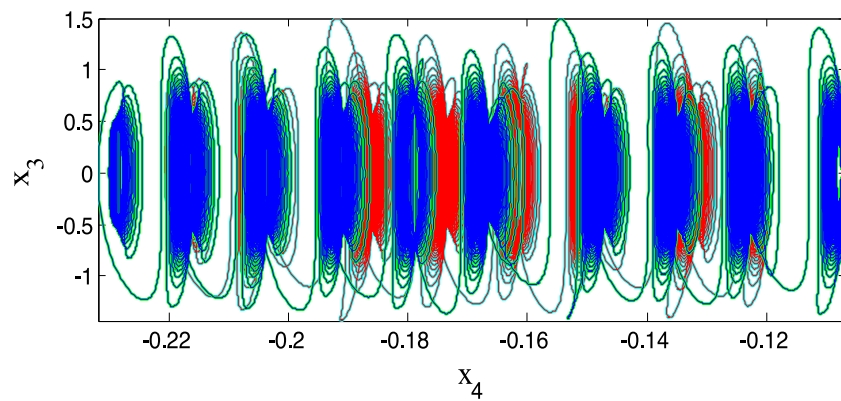


Fig. 8. Coexistence of multiple attractors (ten and eight) of the fifth Case (QS5), with $x(0) = (\pm 0.01, 0.01, 0.01, \pm 0.01)^T$, $2000 < T < 4000$ and $c = 0.01$.

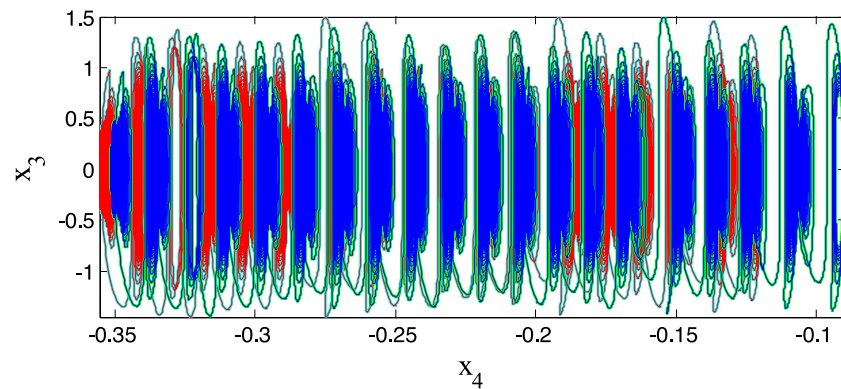


Fig. 9. Coexistence of multiple attractors (twenty) of the fifth Case (QS5), with $x(0) = (\pm 0.01, 0.01, 0.01, \pm 0.01)^T$, $1800 < T < 6000$ and $c = 0.01$.

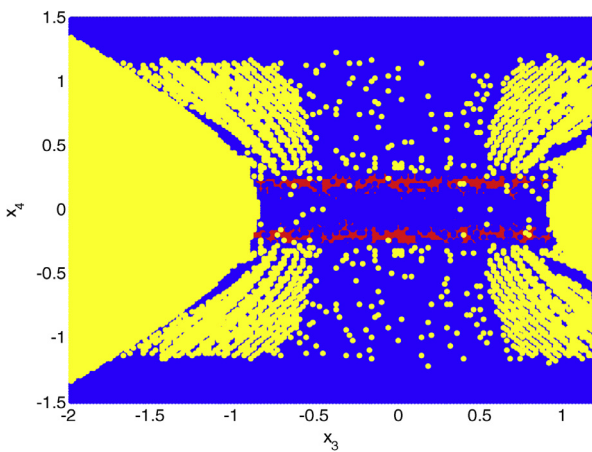


Fig. 10. Basin of attraction with $x_1 = x_2 = 0$ and $h = 5$, $d = 3$, $g = 1$, $1/a^2 = 2.5$, $b = 1$, $1/c^2 = 2.5$ of Case QS4 where colour with red is hyperchaotic, blue is chaotic, and yellow is unbounded and other behaviour. (For interpretation of the references to colour in this figure legend, the reader is referred to the web version of this article.)

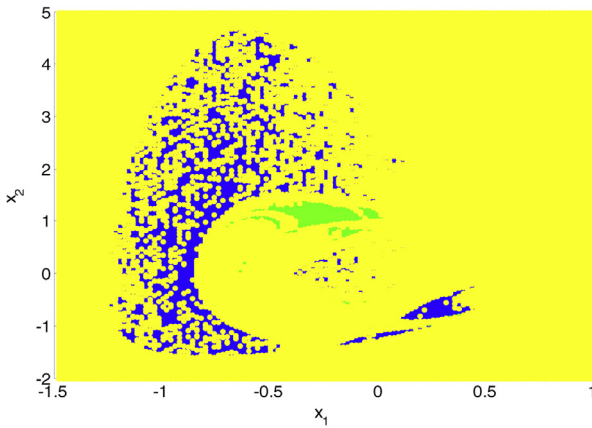


Fig. 11. Basin of attraction with $x_3 = x_4 = 0$ and $h = 5$, $d = 3$, $g = 1$, $1/a^2 = 2.5$, $b = 1$, $1/c^2 = 2.5$ of Case QS4 where colour in blue is chaotic, green is periodic, and yellow is unbounded and other behaviour. (For interpretation of the references to colour in this figure legend, the reader is referred to the web version of this article.)

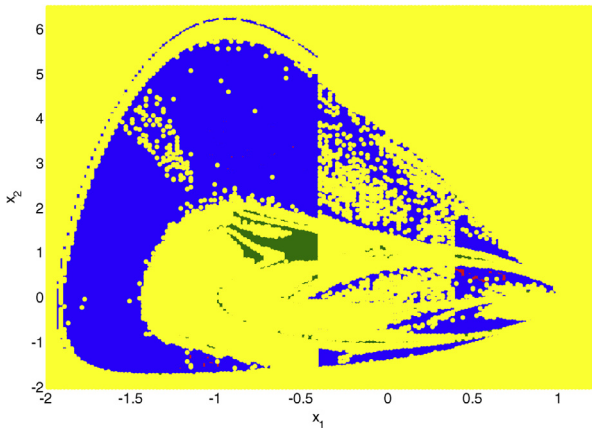


Fig. 12. Basin of attraction with $x_3 = x_4 = 0$ and $h = 5$, $d = 3$, $g = 0.01$, $a = 1$, $b = 1$ of Case QS5 where colour with red is hyperchaotic, blue is chaotic, green is periodic, and yellow is unbounded and other behaviour. (For interpretation of the references to colour in this figure legend, the reader is referred to the web version of this article.)

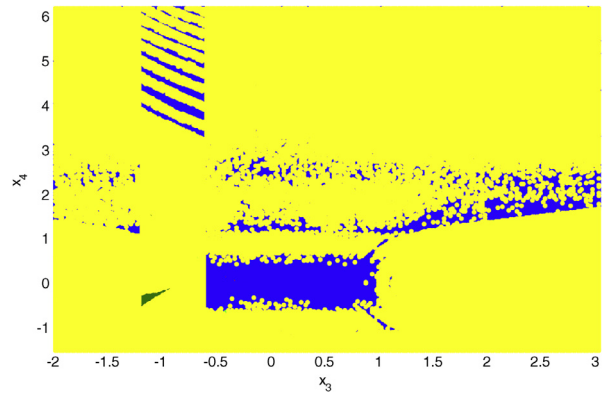


Fig. 13. Basin of attraction with $x_1 = x_2 = 0$ and $h = 5$, $d = 3$, $g = 0.01$, $a = 1$, $b = 1$ of Case QS5 where colour with red is hyperchaotic, blue is chaotic, green is periodic, and yellow is unbounded and other behaviour. (For interpretation of the references to colour in this figure legend, the reader is referred to the web version of this article.)

vation time and sufficiently smaller sampling size [54]. According to the definition [52], Lyapunov exponents are defined in the limit $t \rightarrow \infty$. Thus, the convergence of the LEs is expected to reach their steady values when a large observation time is considered. As discussed in [52], Lyapunov exponents involve long time average behaviour [52]. A short segment of a system trajectories cannot be expected to accurately produce the exact sign of Lyapunov exponents [52,55]. Lyapunov spectrums of the systems are calculated by using the Wolf algorithm [52], with initial conditions $x(0) = (0.01, 0.01, 0.01, 0.01)^T$, and sampling size $\Delta t = 0.1$ and observation time $T = 30,000$ in MATLAB simulation environment. In MATLAB, time variable is defined as $T = 0 : \Delta t : 3000$, where T is the total observation time and Δt is the sampling time. Using ‘tic’ and ‘toc’ command in MATLAB, it is found that the actual time for the calculation of Lyapunov exponents for a sets of parameter is approximately 3 minutes. A discussion on the reliable computation time for a chaotic system can be seen in [56]. It is seen from Figs. 4 and 5 that QS1 Case has hyperchaotic, chaotic and periodic behaviours but Case QS2 has only chaotic behaviour. Case QS1 has hyperchaotic behaviour in the range of $2.615 < \frac{1}{a^2} < 3.025$. Here, the Lyapunov spectrums of the cases are shown with the variation of one parameter only.

We know hyperchaotic/chaotic systems are highly sensitive to initial conditions and value of their parameters. Hence, with the change of initial conditions and parameters values, response of a chaotic/hyperchaotic system changes drastically. For example, Lyapunov spectrum with the variation of parameter a of Case QS1 is shown in Fig. 4. Here, it can be observed that Case QS1 has different behaviours according to the sign of Lyapunov exponents $(+, 0, -, -)$ for chaotic behaviour, $(+, +, 0, -)$ for hyperchaotic behaviour, $(0, 0, -, -)$ for periodic behaviour for different values of parameter. Thus, we observe different behaviours with the variation of parameters.

It may be noted here that all the parameters of a system can be varied to obtain the maximum values of Lyapunov exponents using some soft computing techniques [57,58].

The coexistence of chaotic attractors for all cases of the proposed systems is shown in Fig. 3. It has also been noted that most of these cases have some special behaviours like coexistence of different type of attractors. Some of these are shown in this paper.

The coexistence of periodic behaviours of Case QS1 with $1/a^2 = 4.5$ is shown in Fig. 6. The coexistence of periodic orbits, and coexistence of a periodic orbit and an infinitely going trajectory for Case QS4 with $1/a^2 = 4.85$ are shown in Fig. 7. It is observed from Fig. 7a that with the initial conditions

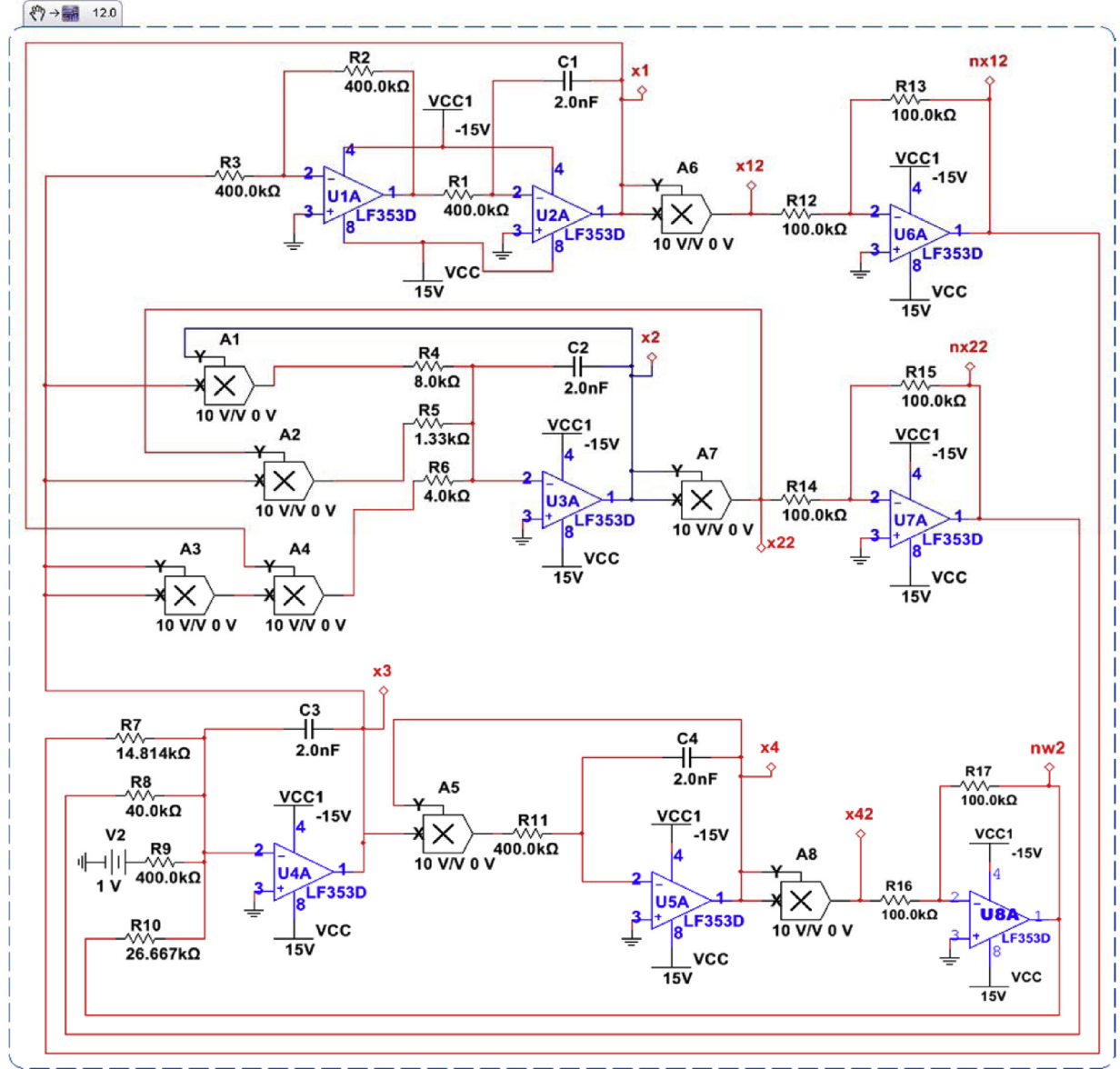


Fig. 14. Circuit of Case QS1.

$x(0) = (\pm 0.1, 0.01, \pm 0.01, 0.1)^T$, Case QS4 has coexistence of periodic orbits. But, with $x(0) = (\pm 0.01, 0.01, \pm 0.01, 0.1)^T$ initial conditions, Case QS4 has coexistence of a periodic orbit and a trajectory going to infinity (Fig. 7b). This is shown to highlight the high sensitivity of the initial conditions. This example shows that with some initial conditions, the system has periodic behaviour and with a change in the sign of one initial condition, the system has unbounded responses, i.e. trajectories going to infinity.

The coexistence of chaotic attractors of QS5 Case is shown in Figs. 8 and 9. It is seen from Figs. 8 and 9 that the number of attractors of Case QS5 increases with the increase in the observation time. Thus, we can say that QS5 Case may exhibit an infinite number of attractors with an increase in time.

The basin of attractions of Cases QS4 and QS5 are shown in Figs. 10, 11 12, and 13, respectively. Here, the basin of attraction of the Cases is generated by finding Lyapunov exponents corresponding to each point and recorded with a separate colour for each behaviour. It is seen from Figs. 10–13 that the Cases have coexistence of attractors. The systems with coexisting attractors may have ridged basin or fractals basin of attraction [59–62].

5. Circuit design and implementation

This section describes the circuit design and realisation of QS1, QS5 and QQ6 Cases. Other cases are not considered to avoid repetition and can be done by similar approaches.

Circuit realisation of a chaotic/hyperchaotic system represents its real applicability [63–67]. Circuit realisation of chaotic systems are used in many applications like secure communication [68–70], random number generator [71], autonomous mobile robot [72], information theory [65,69,73,74], etc. Circuit realisation of various chaotic/hyperchaotic systems are achieved by FPGA tool [69,70,73,75], Cadence OrCAD [67,76] and NI Multisim [77–81] circuit simulation software. In this paper, the circuit realisation of the new systems (4)–(5) for QS1, QS5 and QQ6 Cases are achieved using NI Multisim 12 software. The circuit implementation results obtained by using Multisim software are generally consistent with the actual circuit results [78]. The designed circuit of QS1 Case is shown in Fig. 14. The circuit (Fig. 14) has four integrators (U2A–U5A) to realise four states of Case QS1. The circuit consists of four capacitors (C1, C2, C3, C4), seventeen resistances (R1,..., R17), eight

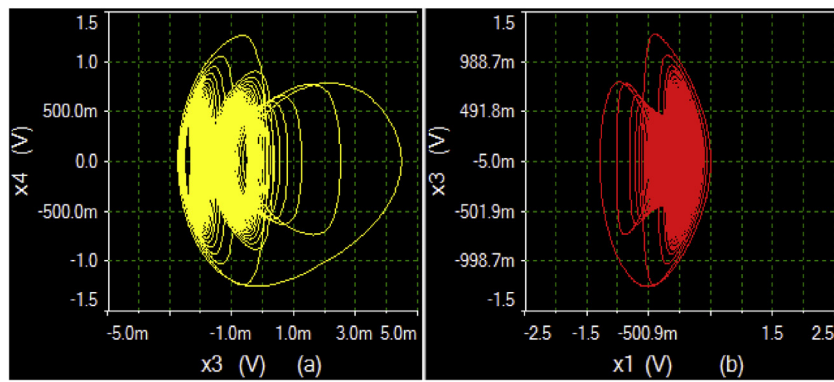


Fig. 15. Attractors of Case QS1 obtained using circuit implementation.

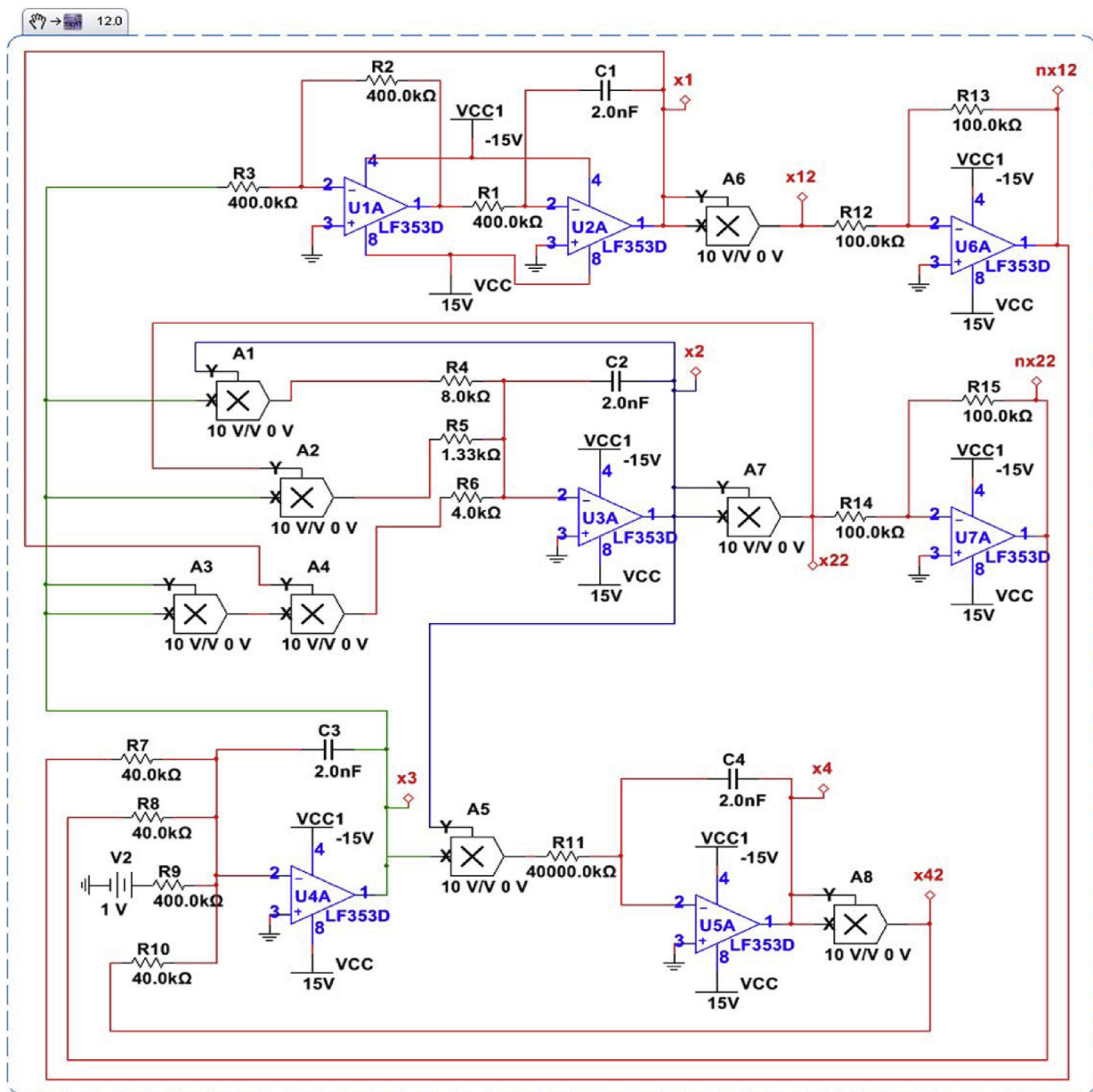


Fig. 16. Designed circuit of Case QS5.

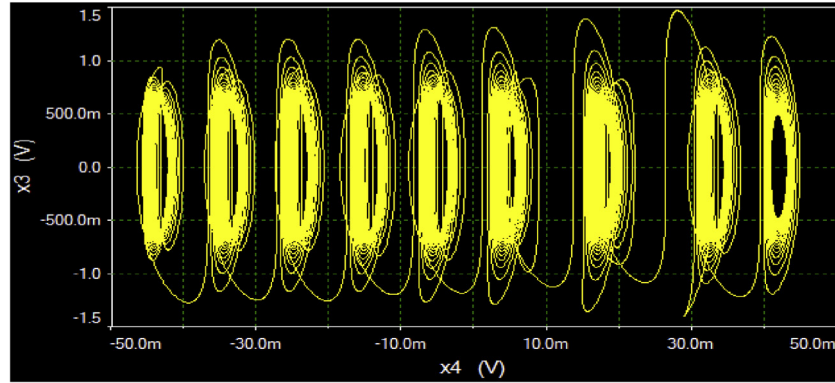


Fig. 17. Attractors of Case QS5 obtained using circuit implementation.

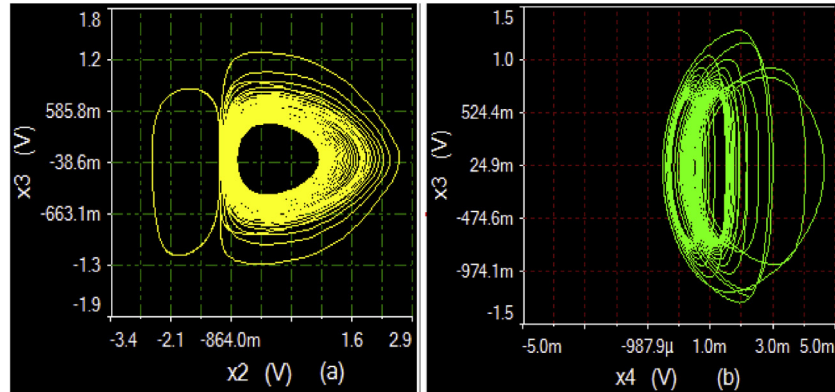


Fig. 18. Attractors of Case QS6 obtained using circuit implementation.

Op-Amp (LF353D) and eight multipliers (AD633). The multipliers (AD633) are used to realise nonlinear terms. The circuit equations of Case QS1 can be written using Kirchhoff's laws as:

$$\begin{cases} \dot{x}_1 = \frac{1}{RC_1} \left[\frac{R}{R_1} x_3 \right] \\ \dot{x}_2 = \frac{1}{RC_2} \left[-\frac{0.1R}{R_4} x_2 x_3 - \frac{0.01R}{R_5} x_2^2 x_3 - \frac{0.01R}{R_6} x_1 x_3^2 \right] \\ \dot{x}_3 = \frac{1}{RC_3} \left[\frac{0.1R}{R_7} x_1^2 + \frac{0.1R}{R_8} x_2^2 + \frac{0.1R}{R_{10}} x_4^2 - \frac{R}{R_9} V_2 \right] \\ \dot{x}_4 = \frac{1}{RC_4} \left[-\frac{0.1R}{R_{11}} x_3 x_4 \right] \end{cases} \quad (10)$$

where the variables x_1, x_2, x_3, x_4 are the outcome of U2A, U3A, U4A and U5A, respectively. System (10) is equivalent to QS1 Case, given in Table 2, with $\tau = t/RC$, $R_1 = R_2 = R_3 = R_9 = 400$ kΩ, $R_4 = \frac{0.1R}{h} = 8.0$ kΩ, $R_5 = \frac{0.01R}{d} = 1.33$ kΩ, $R_6 = 0.01R = 4.0$ kΩ, $R_7 = 0.1a^2R = 14.81$ kΩ, $R_8 = 0.1b^2R = 40.0$ kΩ, $R_{10} = 0.1c^2R = 26.667$ kΩ, $R_{11} = gR = 400$ kΩ, $C_1 = C_2 = C_3 = C_4 = 2$ nF, $\frac{1}{a^2} = 1$, $\frac{1}{b^2} = 1$, $h = 5$, $d = 3$, $g = 1$. Chaotic attractors of Case QS1 obtained using circuit implementation are shown in Fig. 15.

The circuit design for the implementation of Case QS5 is shown in Fig. 16. The designed circuit (Fig. 16) has the same number of components as used in the circuit design of Case QS1 (Fig. 14). The circuit equations of Case QS5 obtained using Kirchhoff's laws can be written as:

$$\begin{cases} \dot{x}_1 = \frac{1}{RC_1} \left[\frac{R}{R_1} x_3 \right] \\ \dot{x}_2 = \frac{1}{RC_2} \left[-\frac{0.1R}{R_4} x_2 x_3 - \frac{0.01R}{R_5} x_2^2 x_3 - \frac{0.01R}{R_6} x_1 x_3^2 \right] \\ \dot{x}_3 = \frac{1}{RC_3} \left[\frac{0.1R}{R_7} x_1^2 + \frac{0.1R}{R_8} x_2^2 - \frac{0.1R}{R_{10}} x_4^2 - \frac{R}{R_9} V_2 \right] \\ \dot{x}_4 = \frac{1}{RC_4} \left[-\frac{0.1R}{R_{11}} x_2 x_3 \right] \end{cases} \quad (11)$$

where the variables x_1, x_2, x_3, x_4 are the outcome of the U2A, U3A, U4A and U5A, respectively. System in (11) is equivalent to QS5 Case, given in Table 2, with $\tau = t/RC$, $R_1 = R_2 = R_3 = R_9 = 400$ kΩ,

$R_4 = \frac{0.1R}{h} = 8.0$ kΩ, $R_5 = \frac{0.01R}{d} = 1.33$ kΩ, $R_6 = 0.01R = 4.0$ kΩ, $R_7 = 0.1a^2R = 40.0$ kΩ, $R_8 = 0.1a^2R = 40.0$ kΩ, $R_{10} = 0.1b^2R = 40.0$ kΩ, $R_{11} = gR = 40,000$ kΩ, $C_1 = C_2 = C_3 = C_4 = 2$ nF, $\frac{1}{a^2} = 1$, $\frac{1}{b^2} = 1$, $h = 5$, $d = 3$, $g = 0.01$. Chaotic attractors of QS5 Case obtained using circuit implementation are shown in Fig. 17. It is seen from Fig. 17 that the attractor plots of Case QS5 obtained using circuit implementation matches with the MATLAB simulation results (Fig. 3). The circuit design and implementation of Case QS6 is also done. The attractor plots of Case QS6 which are generated by circuit implementation are shown in Fig. 18. These attractors confirm the MATLAB simulation results.

6. Conclusions

In this paper, a family of 4-D hyperchaotic/chaotic systems is reported. The family has three systems including three hyperchaotic and five chaotic cases with different shapes of quadric surfaces of equilibria. Six of the cases in proposed systems have non-degenerate quadric surfaces (ellipsoid, paraboloid, and hyperboloid) of equilibria and two of the cases in the proposed system have the degenerate quadric surfaces (cylinder) type of equilibria. With the change in initial conditions, all the cases in the new systems show coexistence of chaotic attractors i.e. multistability behaviours. Case QS5 has coexistence of an infinite number of attractors. Coexistence of periodic orbits, and coexistence of periodic orbit and an infinitely increasing trajectory are observed in Case QS4. Saddle point and non-hyperbolic type of equilibria are observed in Case QS1, QS5 and QS7. MATLAB simulations confirm various claims about these proposed systems. The circuit implementations of Cases QS1, QS5 and QS6 of the new systems validates the MATLAB simulation results and their real applicability. Generation of some new higher dimensional hyperchaotic systems with

unique properties and maximisation of their Lyapunov exponents using soft computing techniques are reserved as the future directions of the paper.

References

- [1] Jafari S, Sprott JC, Pham V, Volos C, Li C. Simple chaotic 3D flows with surfaces of equilibria. *Nonlinear Dyn* 2016;86:1349–58.
- [2] Kiseleva M, Kondratyeva N, Kuznetsov N, Leonov G. Hidden oscillations in electromechanical systems. In: Dynamics and control of advanced structures and machines. Berlin Heidelberg: Springer-Verlag; 2017. p. 119–24. doi:10.1007/978-3-319-43080-5.
- [3] Pham V, Volos C, Jafari S, Vaidyanathan S, Kapitaniak T, Wang X. A chaotic system with different families of hidden attractors. *Int J Bifurc Chaos* 2016;26:1650139–48.
- [4] Kingni ST, Jafari S, Pham V-T, Woaf P. Constructing and analysing of a unique three-dimensional chaotic autonomous system exhibiting three families of hidden attractors. *Math Comput Simul* 2016;132:172–82.
- [5] Pham V-T, Jafari S, Wang X. A chaotic system with different shapes of equilibria. *Int J Bifurc Chaos* 2016;26:1650069–75.
- [6] García-Martínez M, Otañón-García LJ, Campos-Cantón E, Čelikovský S. Hyperchaotic encryption based on multi-scroll piecewise linear systems. *Appl Math Comput* 2015;270:413–24. doi:10.1016/j.amc.2015.08.037.
- [7] Otañón-García LJ, Campos-Cantón E, Femat R. Analog electronic implementation of a class of hybrid dissipative dynamical system. *Int J Bifurc Chaos* 2016;26:1650018–30. doi:10.1142/S0218127416500188.
- [8] Otañón-García LJ, Jiménez-López E, Campos-Cantón E, Basin M. A family of hyperchaotic multi-scroll attractors in Rn. *Appl Math Comput* 2014;233:522–33. doi:10.1016/j.amc.2014.01.134.
- [9] Escalante-González RJ, Campos-Cantón E, Nicol M. Generation of multi-scroll attractors without equilibria via piecewise linear systems. *Chaos* 2017;27:053109–14. doi:10.1063/1.4983523.
- [10] Leonov GA, Kuznetsov NV, Vagaitsev VI. Localization of hidden Chua attractors. *Phys Lett A* 2011;375:2230–3.
- [11] Leonov GA, Kuznetsov NV, Kuznestova OA, Seledzhi SM, Vagaitsev VI. Hidden oscillations in dynamical systems system. *Trans Syst Control* 2011;6:1–14.
- [12] Leonov GA, Kuznetsov NV, Vagaitsev VI. Hidden attractor in smooth Chua systems. *Phys D* 2012;241:1482–6.
- [13] Lorenz EN. Deterministic nonperiodic flow. *J Atmos Sci* 1963;20:130–41.
- [14] Rössler OE. An equation for continuous chaos. *Phys Lett A* 1976;57:397–8.
- [15] Lü J, Chen G, Cheng D, Celikovsky S. Bridge the gap between the Lorenz system and the Chen system. *Int J Bifurc Chaos* 2002;12:2917–26.
- [16] Singh PP, Singh JP, Roy BK. Synchronization and anti-synchronization of Lu and Bhalekar-Gejji chaotic systems using nonlinear active control. *Chaos Solitons Fractals* 2014;69:31–9. doi:10.3182/20140313-3-IN-3024.00069.
- [17] Singh JP, Roy BK. Crisis and inverse crisis route to chaos in a new 3-D chaotic system with saddle, saddle foci and stable node foci nature of equilibria. *Optik (Stuttgart)* 2016;127:11982–2002.
- [18] Kingni ST, Jafari S, Simo H, Woaf P. Three-dimensional chaotic autonomous system with only one stable equilibrium: analysis, circuit design, parameter estimation, control, synchronization and its fractional-order form. *Eur Phys J Plus* 2014;129:1–16.
- [19] Tahir FR, Jafari S, Pham V-T, Volos C, Wang X. A novel no-equilibrium chaotic system with multiwing butterfly attractors. *Int J Bifurc Chaos* 2015;25:1550056–1550067.
- [20] Pham V-T, Volos C, Jafari S, Kapitaniak T. Coexistence of hidden chaotic attractors in a novel no-equilibrium system. *Nonlinear Dyn* 2016;1:1–10. doi:10.1007/s11071-016-3170-x.
- [21] Leonov GA, Kuznetsov NV. Hidden attractors in dynamical systems: from hidden oscillations in Hilbert-Kolmogorov, Aizerman, and Kalman problems to hidden chaotic attractor in Chua circuits. *Int J Bifurc Chaos* 2013;23:1330002–1330071.
- [22] Leonov GA, Kuznetsov NV, Kiseleva MA, Solovyeva EP, Zaretskiy AM. Hidden oscillations in mathematical model of drilling system actuated by induction motor with a wound rotor. *Nonlinear Dyn* 2014;77:277–88.
- [23] Pham VT, Jafari S, Volos C, Giakoumis A, Vaidyanathan S, Kapitaniak T. A chaotic system with equilibria located on the rounded square loop and its circuit implementation. *IEEE Trans Circuits Syst II Express Briefs* 2016;63:878–82.
- [24] Dudkowski D, Jafari S, Kapitaniak T, Kuznetsov NV, Leonov GA, Prasad A. Hidden attractors in dynamical systems. *Phys Rep* 2016;637:1–50.
- [25] Jafari S, Sprott JC. Erratum: simple chaotic flows with a line equilibrium (Chaos, Solitons and Fractals (2013) 57 (79–84)). *Chaos Solitons Fractals* 2015;77:341–2.
- [26] Jafari S, Sprott JC. Simple chaotic flows with a line equilibrium. *Chaos, Solitons Fractals* 2013;57:79–84. doi:10.1016/j.chaos.2013.08.018.
- [27] Wang X, Chen G. Constructing a chaotic system with any number of equilibria. *Nonlinear Dyn* 2012;71:429–36.
- [28] Goethans T, Petrela J. New class of chaotic systems with circular equilibrium. *Nonlinear Dyn* 2015;81:1143–9.
- [29] Kingni ST, Pham V-T, Jafari S, Kol GR, Woaf P. Three-Dimensional chaotic autonomous system with a circular equilibrium: analysis, circuit implementation and its fractional-order form. *Circuits Syst Signal Process* 2016;35:1807–13.
- [30] Goethans T, Sprott JC, Petrela J. Simple chaotic flow with circle and square equilibrium. *Int J Bifurc Chaos* 2016;26:1650137–45.
- [31] Barati K, Jafari S, Sprott JC, Pham V. Simple chaotic flows with a curve of equilibria. *Int J Bifurc Chaos* 2016;26:1630034–40.
- [32] Pham V-T, Jafari S, Volos C, Vaidyanathan S, Kapitaniak T. A chaotic system with infinite equilibria located on a piecewise linear curve. *Optik (Stuttgart)* 2016;127:9111–17.
- [33] Pham V-T, Jafari S, Volos C, Giakoumis A, Vaidyanathan S, Kapitaniak T. A chaotic system with equilibria located on the rounded square loop and its circuit implementation. *IEEE Trans Circuits Syst II Express Briefs* 2016;63:878–82.
- [34] Qi G, Chen G. A spherical chaotic system. *Nonlinear Dyn* 2015;81:1381–92.
- [35] Jafari S, Sprott JC, Molaie M. A simple chaotic flow with a plane of equilibria. *Int J Bifurc Chaos* 2016;26:1650098–104.
- [36] Zhou P, Yang F. Hyperchaos, chaos, and horseshoe in a 4D nonlinear system with an infinite number of equilibrium points. *Nonlinear Dyn* 2014;76:473–80.
- [37] Li C, Sprott JC, Thio W. Bistability in a hyperchaotic system with a line equilibrium. *J Exp Theor Phys* 2014;118:494–500.
- [38] Chen Y, Yang Q. A new Lorenz-type hyperchaotic system with a curve of equilibria. *Math Comput Simul* 2015;112:40–55.
- [39] Ma J, Chen Z, Wang Z, Zhang Q. A four-wing hyper-chaotic attractor generated from a 4-D memristive system with a line equilibrium. *Nonlinear Dyn* 2015;81:1275–88.
- [40] Li Q, Hu S, Tang S, Zeng G. Hyperchaos and horseshoe in a 4D memristive system with a line of equilibria and its implementation. *Int J Circuit Theory Appl* 2014;42:1172–88.
- [41] Gilardi-Velázquez HE, Otañón-García LJ, Hurtado-Rodriguez DG, Campos-Cantón E. Multistability in piecewise linear systems by means of the eigen-spectra variation and the round function. *Int J Bifurc Chaos* 2017;27:1730031–45. doi:10.1142/S0218127417300312.
- [42] Pham V, Jafari S, Volos C, Kapitaniak T. A gallery of chaotic systems with an infinite number of equilibrium points. *Chaos Solitons Fractals* 2016;93:58–63.
- [43] Venit S, Bishop W. Elementary linear algebra. 4th ed. International Thompson Publishing; 1996.
- [44] Sprott JC. Some simple chaotic flow. *Phys Rev E* 1994;50:647–50.
- [45] Iooss G, Helleman RH, Stora R. Chaotic behaviour of deterministic systems. *Chaotic Behav Determin Syst Les Houches Sess* 1983;XXXVI:455–510. doi:10.1017/CBO9780511608162.
- [46] Sprott JC. Elegant chaos, algebraically simple chaotic flows. World Scientific Publishing Co. Pte. Ltd.; 2010.
- [47] Sprott JC. Simple chaotic systems and circuits. *Am J Phys* 2000;68:758–63.
- [48] Sprott JC. Automatic generation of strange attractors. *Comput Graph* 1993;17:325–32.
- [49] Munmuangsaen B, Srisuchinwong B, Sprott JC. Generalization of the simplest autonomous chaotic system. *Phys Lett A* 2011;375:1445–50.
- [50] Khan SA. Quadratic surfaces in science and engineering. *Indian Assoc Phys Teach* 2010;2:327–30.
- [51] Andrilli S, Hecker D. Elementary linear algebra, 9. 4th ed. Burlington, USA: Academic Press is an imprint of Elsevier; 2010. doi:10.1016/0955-7997(92)90033-4.
- [52] Wolf A, Swift JB, Swinney HL, Vastano JA. Determining Lyapunov exponents from a time series. *Phys D* 1985;16:285–317. doi:10.1016/0167-2789(85)90011-9.
- [53] Sano M, Sawada Y. Measurement of the Lyapunov spectrum from a chaotic time series. *Phys Rev Lett* 1985;55:1082–5. doi:10.1103/PhysRevLett.55.1082.
- [54] Rosenstein MT, Collins JJ, De Luca CJ. A practical method for calculating largest Lyapunov exponents from small data sets. *Phys D Nonlinear Phenom* 1993;65:117–34. doi:10.1016/0167-2789(93)90009-P.
- [55] Singh JP, Roy BK. The nature of Lyapunov exponents is (+, +, −, −). Is it a hyperchaotic system? *Chaos Solitons Fractals* 2016;92:73–85.
- [56] Liao SJ, Wang PF. On the mathematically reliable long-term simulation of chaotic solutions of Lorenz equation in the interval [0,10000]. *Sci China Phys Mech Astron* 2014;57:330–5. doi:10.1007/s11433-013-5375-z.
- [57] Carbalj-Gómez VH, Tlelo-Cuautle E, Fernández FV. Optimizing the positive Lyapunov exponent in multi-scroll chaotic oscillators with differential evolution algorithm. *Appl Math Comput* 2013;219:8163–8. doi:10.1016/j.amc.2013.01.072.
- [58] Fraga LGdela, Tlelo-Cuautle E. Optimizing the maximum Lyapunov exponent and phase space portraits in multi-scroll chaotic oscillators. *Nonlinear Dyn* 2014;76:1503–15. doi:10.1007/s11071-013-1224-x.
- [59] Kapitaniak T. Partially nearly riddled basins in systems with chaotic saddle. *Chaos Solitons Fractals* 2001;12:2363–7.
- [60] Ott E, Alexander JC, Kan I, Sommerer JC, Yorke JA. The transition to chaotic attractors with riddled basins. *Phys D* 1994;76:384–410.
- [61] Sprott JC, Xiong A. Classifying and quantifying basins of attraction. *Chaos* 2015;083101–0831:1–7.
- [62] Heagy JF, Carroll TL, Pecora LM. Experimental and numerical evidence for riddled basins in coupled chaotic systems. *Phys Rev Lett* 1994;73:3528–32.
- [63] Trejo-Guerra R, Tlelo-Cuautle E, Jiménez-Fuentes JM, Sánchez-López C, Muñoz-Pacheco JM, Espinosa-Flores-Verdad G, et al. Integrated circuit generating 3- and 5-scroll attractors. *Commun Nonlinear Sci Numer Simul* 2012;17:4328–35. doi:10.1016/j.cnsns.2012.01.029.
- [64] de la Vega JLVS, Tlelo-Cuautle E. Simulation of piecewise-linear one-dimensional chaotic maps by verilog-A. *IETE Tech Rev* 2015;32:304–10. doi:10.1080/02564602.2015.1018349.
- [65] Nunez JC, Tlelo E, Ramirez C, Jimenez JM. CCII+ Based on QFGMOS for implementing chua chaotic oscillator. *IEEE Lat Am Trans* 2015;13:2865–70. doi:10.1109/LTA.2015.7350032.
- [66] Tlelo-Cuautle E, Pano-Azucena AD, Rangel-Magdaleno JJ, Carbalj-Gómez VH, Rodríguez-Gómez G. Generating a 50-scroll chaotic attractor at 66 MHz by using FPGAs. *Nonlinear Dyn* 2016;85:2143–57. doi:10.1007/s11071-016-2820-3.

- [67] Trejo-Guerra R, Tlelo-Cuautle E, Jiménez-Fuentes M, Muñoz-Pacheco JM, Sánchez-López C. Multiscroll floating gate-based integrated chaotic oscillator. *Int J Circuit Theory Appl* 2011;38:689–708. doi:[10.1002/cta](https://doi.org/10.1002/cta).
- [68] Pano-Azucena AD, de Jesus Rangel-Magdaleno J, Tlelo-Cuautle E, de Jesus Quintas-Valles A. Arduino-based chaotic secure communication system using multi-directional multi-scroll chaotic oscillators. *Nonlinear Dyn* 2017;87:2203–17. doi:[10.1007/s11071-016-3184-4](https://doi.org/10.1007/s11071-016-3184-4).
- [69] Tlelo-Cuautle E, Carbalj-Gómez VH, Obeso-Rodelo PJ, Rangel-Magdaleno JJ, Núñez-Pérez JC. FPGA realization of a chaotic communication system applied to image processing. *Nonlinear Dyn* 2015;82:1879–92. doi:[10.1007/s11071-015-2284-x](https://doi.org/10.1007/s11071-015-2284-x).
- [70] Tlelo-Cuautle E, Rangel-Magdaleno J, de la Fraga LG. *Engineering applications of FPGAs: chaotic systems, artificial neural networks, random number generators, and secure communication systems*. Switzerland: Springer; 2016.
- [71] Valtierra JL, Tlelo-Cuautle E, Rodríguez-Vázquez Á. A switched-capacitor skewtent map implementation for random number generation. *Int J Circuit Theory Appl* 2016;45:305–15. doi:[10.1002/cta.2305](https://doi.org/10.1002/cta.2305).
- [72] Tlelo-Cuautle E, Ramos-López HC, Sánchez-Sánchez M, Pano-Azucena AD, Sánchez-Gaspariano LA, Núñez-Pérez JC, et al. Application of a chaotic oscillator in an autonomous mobile robot. *J Electr Eng* 2014;65:157–62. doi:[10.2478/jee-2014-0024](https://doi.org/10.2478/jee-2014-0024).
- [73] Tlelo-Cuautle E, de Jesus Quintas-Valles A, de La Fraga LG, de Jesus Rangel-Magdaleno J. VHDL descriptions for the FPGA implementation of PWL-function-based multi-scroll chaotic Oscillators 2016;11. doi:[10.1371/journal.pone.0168300](https://doi.org/10.1371/journal.pone.0168300).
- [74] Trejo-Guerra R, Tlelo-Cuautle E, Carbajal-Gómez VH, Rodriguez-Gómez G. A survey on the integrated design of chaotic oscillators. *Appl Math Comput* 2013;219:5113–22. doi:[10.1016/j.amc.2012.11.021](https://doi.org/10.1016/j.amc.2012.11.021).
- [75] Tlelo-Cuautle E, Rangel-Magdaleno JJ, Pano-Azucena AD, Obeso-Rodelo PJ, Nunez-Perez JC. FPGA realization of multi-scroll chaotic oscillators. *Commun Nonlinear Sci Numer Simul* 2015;27:66–80. doi:[10.1016/j.cnsns.2015.03.003](https://doi.org/10.1016/j.cnsns.2015.03.003).
- [76] Kengne J, Jafari S, Njitacke ZT, Yousefi Azar Khanian M, Cheukem A. Dynamic analysis and electronic circuit implementation of a novel 3D autonomous system without linear terms. *Commun Nonlinear Sci Numer Simul* 2017;52:62–76. doi:[10.1016/j.cnsns.2017.04.017](https://doi.org/10.1016/j.cnsns.2017.04.017).
- [77] Xiong L, Lu Y-J, Zhang Y-F, Zhang X-G, Gupta P. Design and hardware implementation of a new chaotic secure communication technique. *PLoS One* 2016;11:1–19. doi:[10.1371/journal.pone.0158348](https://doi.org/10.1371/journal.pone.0158348).
- [78] Ruo-Xun Z, Shi-ping Y. Adaptive synchronisation of fractional-order chaotic systems. *Chin Phys B* 2010;19:1–7. doi:[10.1088/1674-1056/19/2/020510](https://doi.org/10.1088/1674-1056/19/2/020510).
- [79] Lao S, Tam L, Chen H, Sheu L. Hybrid stability checking method for synchronization of chaotic fractional-order systems. *Abstr Appl Anal* 2014;2014:1–11.
- [80] Singh JP, Roy BK. The simplest 4-D chaotic system with line of equilibria, chaotic 2-torus and 3-torus behaviour. *Nonlinear Dyn* 2017;89:1845–62. doi:[10.1007/s11071-017-3556-4](https://doi.org/10.1007/s11071-017-3556-4).
- [81] Singh JP, Lochan K, Kuznetsov NV, Roy BK. Coexistence of single- and multi-scroll chaotic orbits in a single-link flexible joint robot manipulator with stable spiral and index-4 spiral repellor types of equilibria. *Nonlinear Dyn* 2017;1–23. doi:[10.1007/s11071-017-3726-4](https://doi.org/10.1007/s11071-017-3726-4).